Supporting Information

Gradient and multilevel surface modification of Ni-rich layered cathodes by gas penetration for enhanced electrochemical performance

Rui Jiang*, Zhongjia Dai, Yongen Gao, Xikang Zhao, Jianfang Du, Gang Li*, Zexue Du

Research Institute of Petroleum Processing, SINOPEC, Beijing 100083, China

E-mail address: jiangrui.ripp@sinopec.com (R. Jiang); ligang.ripp@sinopec.com (G. Li)

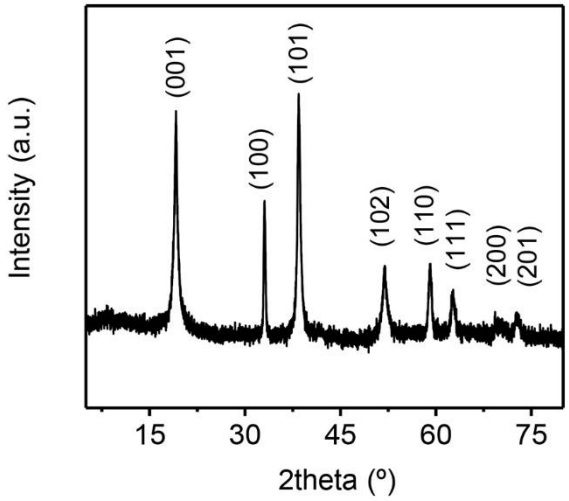

Fig. S1. XRD patterns of the NCM-OH precursor.

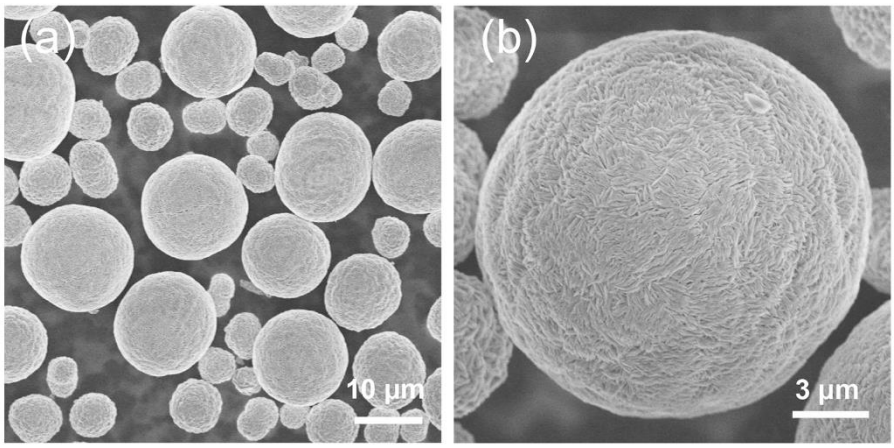

Fig. S2. SEM images of the NCM-OH precursor.

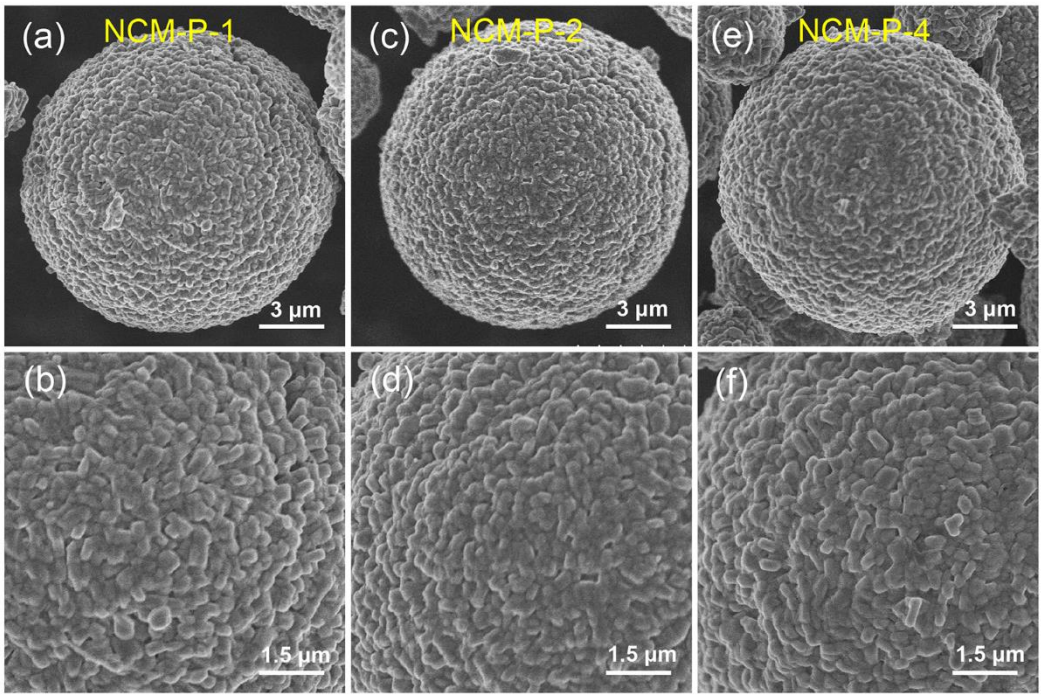

Fig. S3. SEM images of (a, b) NCM-P-1; (c, d) NCM-P-2; (e, f) NCM-P-4.

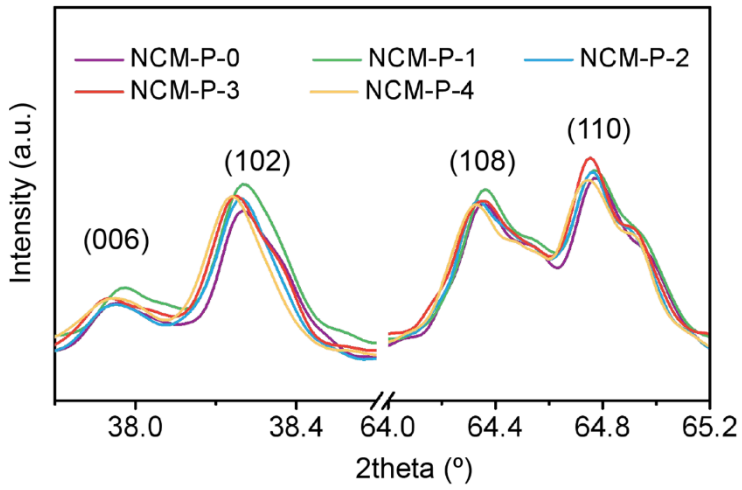

Fig. S4. The partial enlarged XRD patterns of NCM-P-*x* samples.

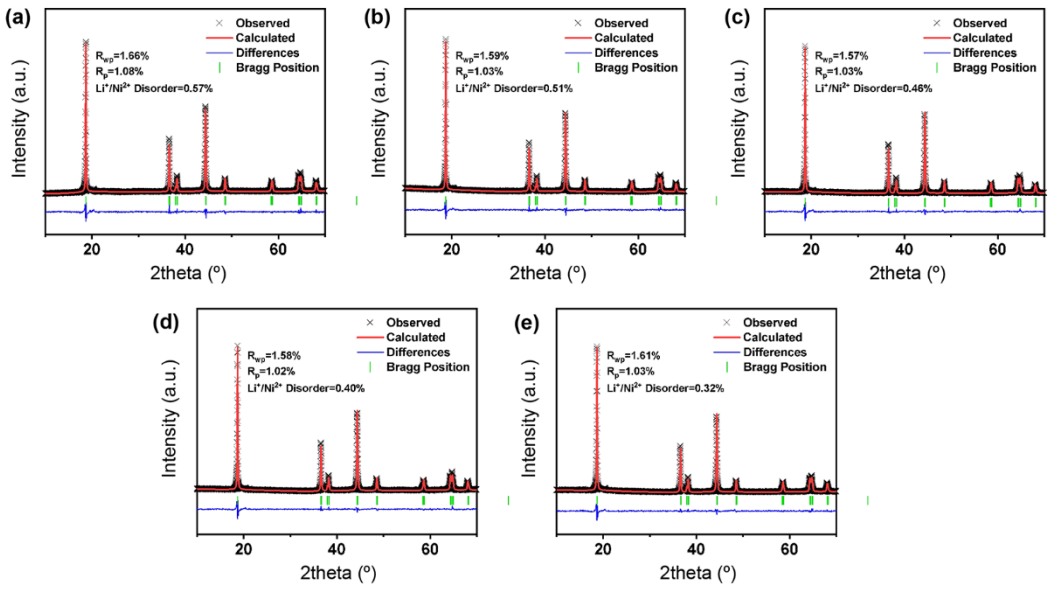

Fig. S5. The XRD refinement of the NCM-P-*x* smaples. (a) NCM-P-0; (b) NCM-P-1; (c) NCM-P-2; (d) NCM-P-3; (e) NCM-P-4.

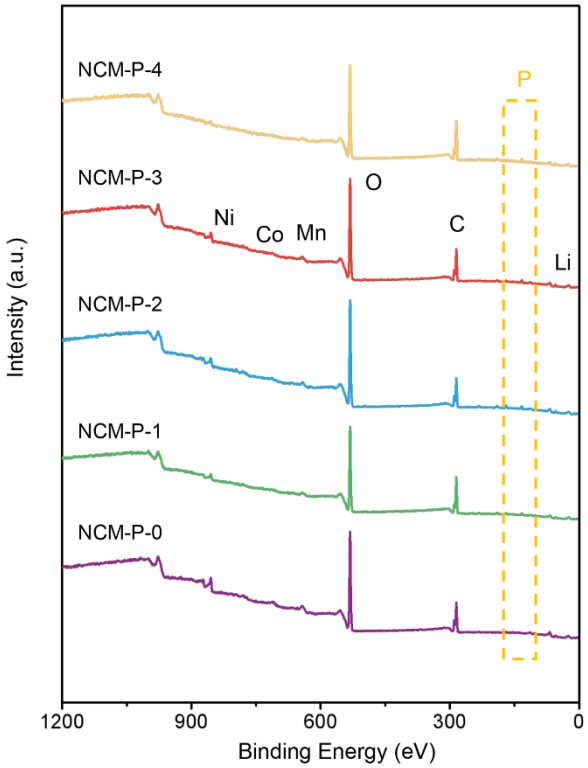

Fig. S6. XPS survey spectra of NCM-P-*x* samples.

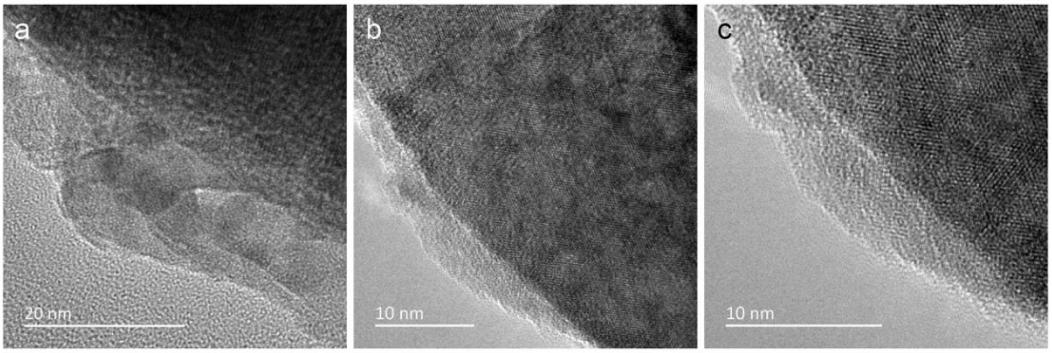

Fig. S7. HRTEM images of NCM-P-3 sample.

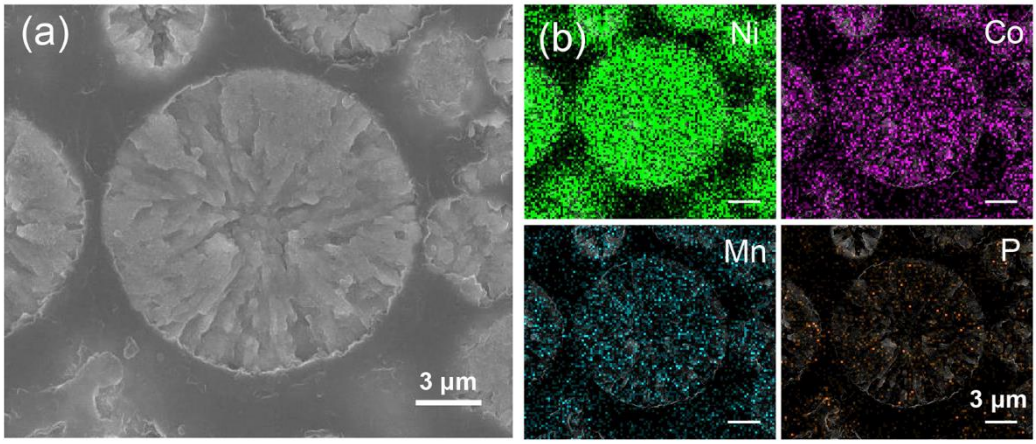

Fig. S8. (a)Cross-sectional SEM images and (b) corresponding element mappings of NCM-P-3.

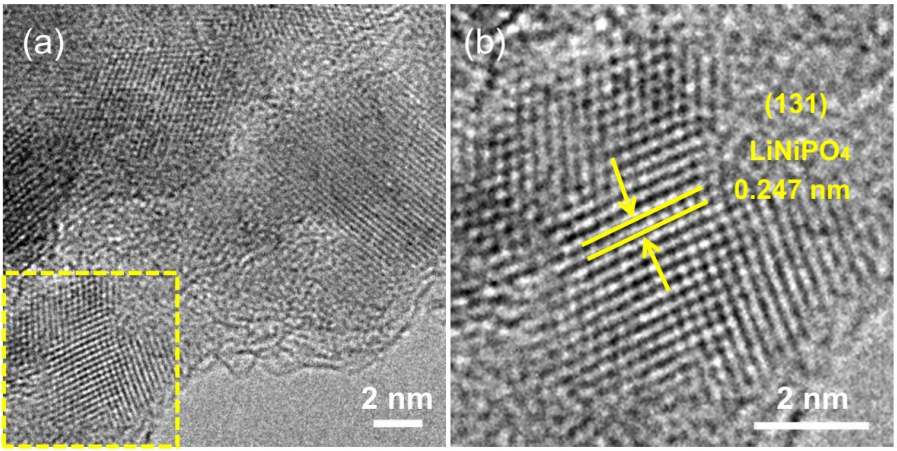

Fig. S9. HRTEM images of the manual pulverized NCM-P-3 sample.

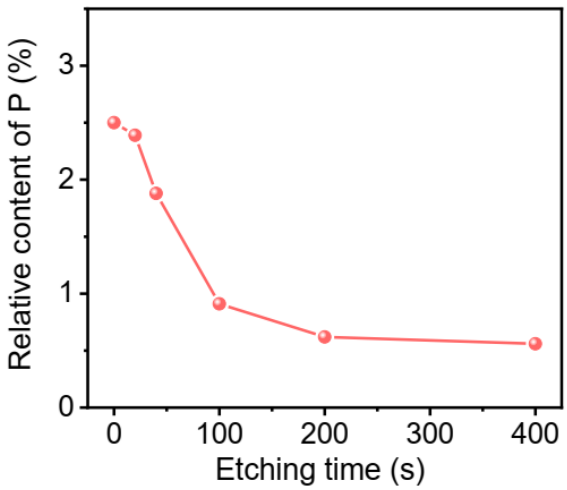

Fig. S10. The relative content of P as a function of etching time based on the XPS depth spectra results.

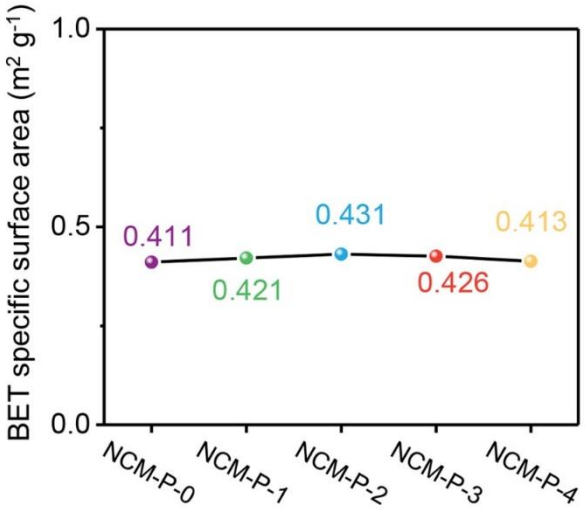

Fig. S11. The BET specific surface area of NCM-P-*x* samples.

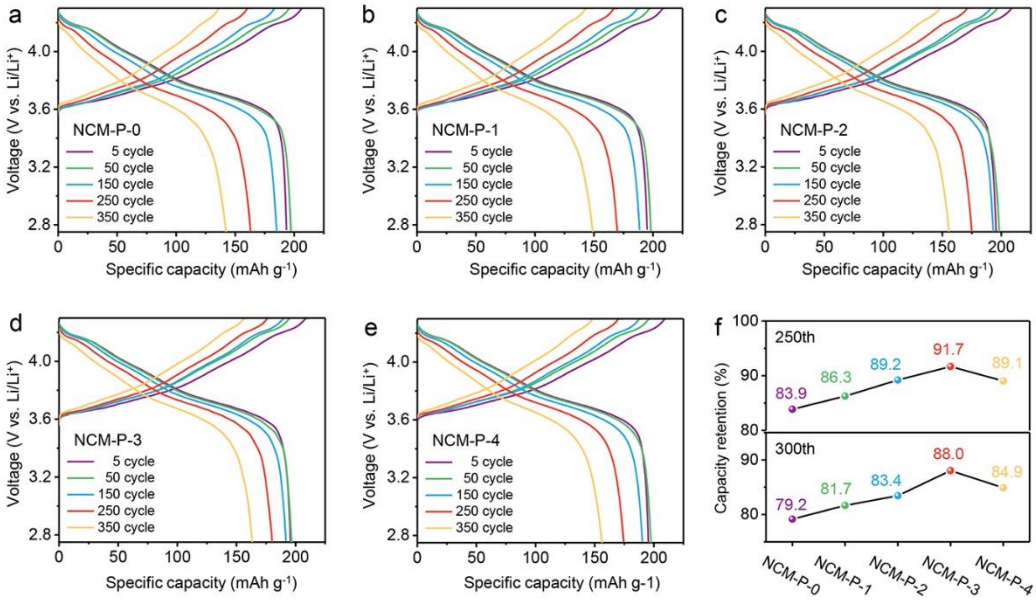

Fig. S12. (a-e) The charge/discharge voltage profile evolution of different cathodes at room temperature. (a) NCM-P-0; (b) NCM-P-1; (c) NCM-P-2; (d) NCM-P-3; (e) NCM-P-4. (f) The capacity retention of NCM-P-*x* after 250 and 300 cycles.

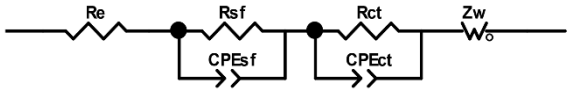

Fig. S13. The relevant equivalent circuit for the EIS measurement of NCM-P-*x* samples.

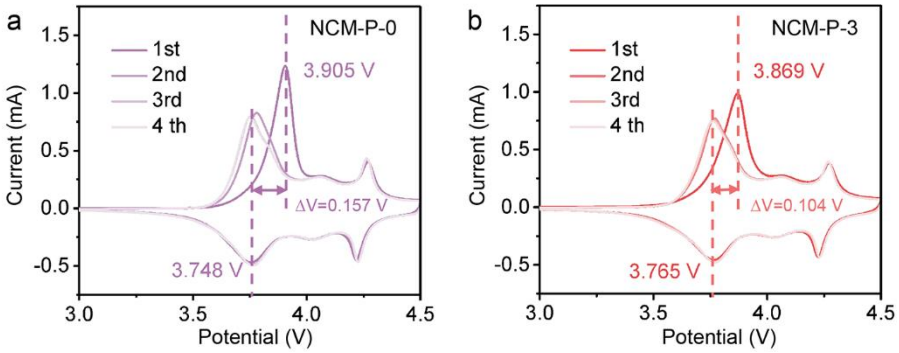

Fig. S14. Cyclic voltammetry curves of (a) NCM-P-0 and (b) NCM-P-3.

Table S1. The intensity ratios of (003)/(104), peak positions, d-spacings of the (003) plane, and lattice parameters of the cathode samples.

Sample	I(003)/I(104)	2Theta(°)	a	d(003)	c
NCM-P-0	1.223	18.735	2.8764	4.7324	14.1972
NCM-P-1	1.250	18.735	2.8764	4.7325	14.1975
NCM-P-2	1.256	18.713	2.877	4.7389	14.2167
NCM-P-3	1.258	18.709	2.8764	4.7391	14.2173
NCM-P-4	1.271	18.696	2.877	4.7423	14.2269

Table S2. The corresponding binding energy positions and area proportion/relative contents for each element from the XPS results.

XPS signals	Bonding energy position (eV)	Area proportion/Relative contents				
		NCM-P-0	NCM-P-1	NCM-P-2	NCM-P-3	NCM-P-4
C 1s – hydrocarbon contaminants (C-H)	284.8	72.4%	77.1%	78.7%	80.3%	80.5%
C 1s – carbonate compounds (CO_3^{2-})	289.7	27.6%	22.9%	21.3%	19.7%	19.5%
P 2p – phosphate ions (PO_4^{3-})	133.4	0	2.13%	2.25%	2.5%	3.01%
Ni 2p – Ni $2p_{3/2}$	855.3	Shifted values of bonding energies				
		0	-0.23	-0.34	-0.46	-0.49

Table S3. The corresponding binding energy positions and area proportion/relative contents for each element from the XPS depth analysis.

XPS signals	Bonding energy position (eV)	Area proportion/Relative contents in the XPS depth analysis				
		0 s	20 s	40 s	100 s	400 s
P 2p – phosphate ions (PO_4^{3-})	133.4	2.50%	2.39%	1.88%	0.89%	0.47%
P 2p – P-M bonds (M= Ni, Co, Mn)	~130	0	0	0	0.02%	0.09%
O 1s – lattice oxygen	529.2	95.2%	76.4%	62.3%	40.9%	32.7%
O 1s – surface impurities	531.9	4.8%	23.6%	37.7%	59.1%	67.3%

Table S4. The detailed cycling performance data of NCM-P-*x* electrodes.

Sample	Specific discharge capacity at 0.5 C (mAh g^{-1})	Specific discharge capacity of the 350th cycles (mAh g^{-1})	The capacity retention of the 350th cycles (%)
NCM-P-0	193.4	139.9	72.3
NCM-P-1	195.1	148.6	76.2
NCM-P-2	195.6	154.5	79.0
NCM-P-3	195.7	162.6	83.1
NCM-P-4	195.4	155.1	79.4

Table S5. Comparison of the cathode materials involved in Li_3PO_4 coatings.

Materials	Methods of the introduction of Li_3PO_4	Capacity retention (%)	References
NCM-P-3	In-situ gas-solid reaction	95.1% after 200 cycles at 0.5C	This work
LPO-infused	ALD coating + annealing	91.6% after 200 cycles at C/3	Nat. Energy 3 (2018) 600–605.
Li_3PO_4–$LiYO_2$@NCM811	Solid mixing + annealing	96.4% after 100 cycles at 1C	J. Alloys Compd. 894 (2021) 162155.
PPy-LP@NCM811	Wet coating + annealing	86.5% after 200 cycles at 1C	ACS Appl. Mater. Interfaces 9 (2017) 29732−29743.
LP@NCM811	Wet coating + annealing	75.7% after 200 cycles at 1C	
Li_3PO_4@NCM622	citric acid assisted sol-gel method	79.7% after 100 cycles at 1C	J. Power Sources 360 (2017) 206−214.
Li_3PO_4–TiO_2@LNMO	ALD coating	89.3% after 100 cycles at 0.5C	Nano Energy, 65 (2019) 103988.
Li_3PO_4 @LNMO	ALD coating	78.4% after 100 cycles at 0.5C	
Li_3PO_4 @NCM811	Solid mixing + annealing	84.6% after 200 cycles at 0.5C	ACS Appl. Energy Mater. 3 (2020) 7445−7455.
Li_3PO_4 @NCM811	Wet absorption + annealing	89.6% after 250 cycles at 1.0 C	Electrochim. Acta 340 (2020) 135871.
Li_3PO_4 @NCM811	Wet mixing + annealing	94.3% after 100 cycles at 0.2C	ACS Appl. Energy Mater. 4 (2021) 2257−2265.

Table S6. Electrochemical impedance fitting results of NCM-P-*x* electrodes after 4 cycles.

Sample	R_{sf}	R_{ct}
NCM-P-0	4.675	27.84
NCM-P-1	3.544	25.17
NCM-P-2	3.243	23.24
NCM-P-3	2.301	20.04
NCM-P-4	2.031	18.96